Nanoelectronics and Its New Materials – A NEW ERA OF NANOSCIENCE

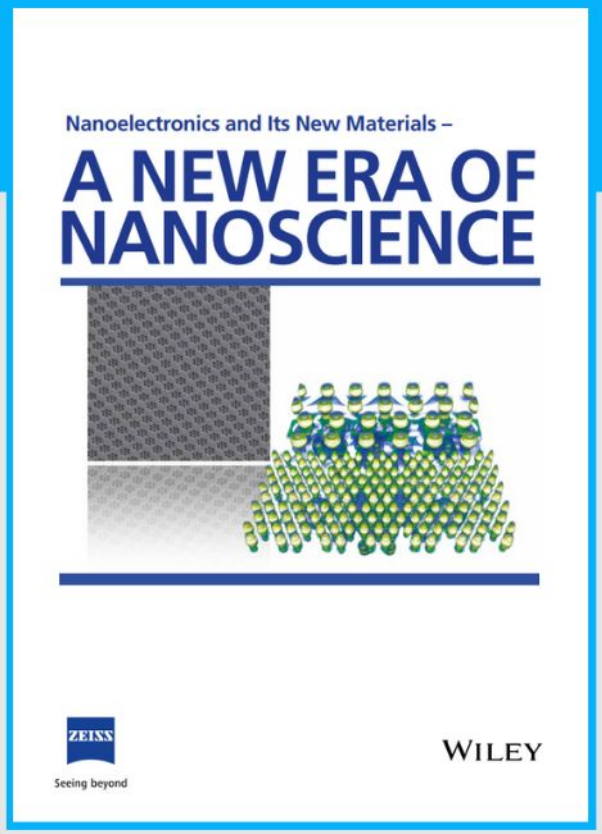

Discover the recent advances in electronics research and fundamental nanoscience.

Nanotechnology has become the driving force behind breakthroughs in engineering, materials science, physics, chemistry, and biological sciences. In this compendium, we delve into a wide range of novel applications that highlight recent advances in electronics research and fundamental nanoscience. From surface analysis and defect detection to tailored optical functionality and transparent nanowire electrodes, this eBook covers key topics that will revolutionize the future of electronics.

To get your hands on this valuable resource and unleash the power of nanotechnology, simply download the eBook now. Stay ahead of the curve and embrace the future of electronics with nanoscience as your guide.

ZEISS

Seeing beyond

WILEY

NANO · MICRO small
www.small-journal.com

Orally-Delivered, Cytokine-Engineered Extracellular Vesicles for Targeted Treatment of Inflammatory Bowel Disease

*Jingang Liu, He Ren, Chen Zhang, Jiexin Li, Qian Qiu, Nan Zhang, Ning Jiang, Jonathan F. Lovell, and Yumiao Zhang**

The use of orally-administered therapeutic proteins for treatment of inflammatory bowel disease (IBD) has been limited due to the harsh gastrointestinal environment and low bioavailability that affects delivery to diseased sites. Here, a nested delivery system, termed Gal-IL10-EVs (C/A) that protects interleukin 10 (IL-10) from degradation in the stomach and enables targeted delivery of IL-10 to inflammatory macrophages infiltrating the colonic lamina propria, is reported. Extracellular vesicles (EVs) carrying IL-10 are designed to be secreted from genetically engineered mammalian cells by a plasmid system, and EVs are subsequently modified with galactose, endowing the targeted IL-10 delivery to inflammatory macrophages. Chitosan/alginate (C/A) hydrogel coating on Gal-IL10-EVs enables protection from harsh conditions in the gastrointestinal tract and favorable delivery to the colonic lumen, where the C/A hydrogel coating is removed at the diseased sites. Gal-IL10-EVs control the production of reactive oxygen species (ROS) and inhibit the expression of proinflammatory cytokines. In a murine model of colitis, Gal-IL10-EVs (C/A) alleviate IBD symptoms including inflammatory responses and disrupt colonic barriers. Taken together, Gal-IL10-EVs (C/A) features biocompatibility, pH-responsive drug release, and macrophage-targeting as a therapeutic platform for oral delivery of bioactive proteins for treating intestinal diseases.

1. Introduction

Crohn's disease and ulcerative colitis, collectively referred to as inflammatory bowel disease (IBD), are a family of chronic, relapsing and debilitating inflammatory disorders, posing a heavy burden on the global healthcare and affecting millions worldwide.[1,2] IBD is typically characterized by disruption of the mucosal barrier,[3] abnormal pH in the affected area,[4] out-of-control oxidative stress response,[5] and inflammation of the colonic lamina propria.[6] The exact etiology and pathogenesis of IBD is still inconclusive, but genetic factors,[7] immune response,[8] environmental and lifestyle factors,[9] and intestinal flora[10] have been shown to be possible contributors to the development of IBD. Traditional treatment options for IBD such as anti-inflammatory drugs or immunosuppressive drugs frequently do not adequately manage IBD symptoms. In addition, their nonspecific effects on the immune system and short or long-term side effects, such as hepatotoxicity, infection susceptibility, and others limit wider clinical use.[11–13]

Whereas antibody therapies directed against tumor necrosis factor-α (TNF-α) and Interleukin-23 are frequently used in steroid-refractory IBD patients, protein-based therapies have emerged as potential treatments because of their high biological selectivity. Interleukin-22,[14] interleukin-13,[15] interleukin-4,[16] and other proteins have been explored for IBD with good therapeutic outcomes. Among them, interleukin-10 (IL-10) is a powerful immunomodulatory cytokine with strong anti-inflammatory, antioxidant, and tissue regenerative properties.[17,18] For the treatment of IBD, many forms of IL-10 formulations have been developed to manage dextran sulfonic (DSS), 2,4,6-trinitrobenzenesulfonic acid, or IL-10$^{-/-}$ gene-induced experimental colitis models in preclinical animal models by limiting proinflammatory factors production and immune cells infiltration,[19,20] showing the potential of IL-10 therapeutics for IBD treatment. However, IL-10 has a short serum half-life (1.1–2.6 h) with chemical and physical instability in circulation, which inevitably activates leukocytes and leads to patient harm and reduced therapeutic efficacy following systemic IL-10 injections.[21,22] Intraperitoneal injection of replication-deficient human type 5 adenoviral vectors bearing an IL-10 gene was used to infect rectal epithelial cells,[23] but concerns about the unknown function of the adenoviral vector and the host antiadenoviral immune response are possible obstacles.[24,25] The oral administration route is the most preferred because of high patient

J. Liu, H. Ren, C. Zhang, J. Li, Q. Qiu, N. Zhang, Y. Zhang
School of Chemical Engineering and Technology
Key Laboratory of Systems Bioengineering (Ministry of Education)
Frontiers Science Center for Synthetic Biology (Ministry of Education)
Tianjin University
Tianjin 300350, P. R. China
E-mail: ymzhang88@tju.edu.cn

N. Jiang
School of Biology and Biological Engineering
South China University of Technology
Guangzhou 510006, P. R. China

J. F. Lovell
Department of Biomedical Engineering
The State University of New York at Buffalo
Buffalo, NY 14260, USA

The ORCID identification number(s) for the author(s) of this article can be found under https://doi.org/10.1002/smll.202304023

DOI: 10.1002/smll.202304023

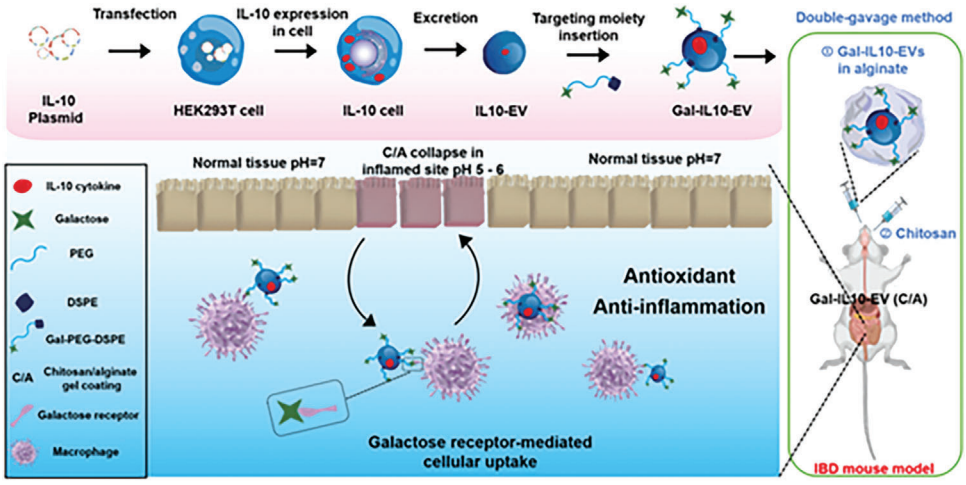

Scheme 1. Schematic illustration of the therapeutic effect of oral Gal-IL10-EVs (C/A) for IBD treatment. HEK293T cells were first genetically engineered to generate IL-10 cytokine-containing extracellular vesicles, followed by galactose insertion and chitosan/alginate coating. Chitosan/alginate hydrogel protects Gal-IL10-EVs to safely pass through the stomach and small intestine before collapse in inflamed colon. Subsequently, the released Gal-IL10-EVs target and act on inflammatory macrophages infiltrating colonic lamina propria.

compliance, but the harsh gastric environment is a major hurdle for the development of protein formulations. Gelatin microspheres containing IL-10[26] or transgenic *Lactococcus lactis*[27,28] have been explored and achieved positive progress, but overall, new approaches for oral delivery of IL-10 for IBD could be beneficial. The challenges include stabilizing IL-10 through the gastric fluids and into the intestinal flora, as well as the biochemical conditions at the diseased site, ultimately aiming for IL-10 enrichment in the vicinity of the target cells. Thus, advanced oral protein formulations are needed to effectively protect and deliver protein drugs with the ability to target specific cells.

Extracellular vesicles (EVs) including exosomes and microvesicles are nanoscale membrane vesicles secreted by mammalian cells in a constitutive or inducible manner.[29,30] EVs can transport different types of functional molecules, including nucleic acids and proteins, to distal or nearby cells to mediate intercellular communication.[31–33] Because of the ability to carry and transfer bioactive molecules, EVs have been proposed as a versatile vehicle for therapeutic delivery.[34,35] Compared with existing delivery systems, EVs are a nonimmunogenic and naturally derived nanovesicle, allowing them to evade phagocytosis and protect their cargo from enzymatic and acidic degradation, resulting in prolonged half-life of therapeutic drugs.[36–39] In addition, the phospholipid membrane structure is enabled subsequent targeted modification; for example, a 1, 2-Distearoyl-sn-glycero-3-phosphoethanolamine (DSPE) moiety with targeting moieties can be anchored on the surface of EV membranes, allowing generation of targeted hybrid EVs.[40,41] Engineered EV-based delivery systems could be an appealing candidate for delivery of IL-10 for IBD treatment, but oral EV delivery systems carrying recombinant proteins have not yet been explored to the best of our knowledge.

In this work, we developed a nested delivery system that orally delivers IL-10 for the treatment of inflammatory bowel disease (**Scheme 1**). The outer coating of the delivery system endows the capability of withstanding the harsh gastric environment, but collapses and responsively releases Gal-IL10-EVs in the pH range of the colonic lumen. Meanwhile, Gal-EVs not only protected IL-10 from proteases and acidic conditions, but also targeted inflammatory macrophages infiltrating the colonic lamina propria to suppress the inflammatory response and restore the disrupted colonic barrier. This work demonstrates the potential for the use of extracellular vesicle for delivery of IL-10 for the treatment of inflammatory bowel disease.

2. Result and Discussions

2.1. Preparation and Characterization of the Gal-IL10-EVs

For the treatment of IBD, we chose IL-10 as the cargo protein because of its powerful immunomodulatory function, and EVs were selected as delivery carriers. To that end, we first constructed a murine IL-10 expression plasmid and an identical empty plasmid control. This was confirmed using colony polymerase chain reaction (PCR). As shown in **Figure 1**A, we demonstrated the presence of 537 bp amplicon in the IL-10 gene in the IL-10 positive plasmid but not in the empty one. In order to generate IL10-loaded EVs (IL10-EVs), the aforementioned IL-10 plasmids were transiently transfected into human embryonic kidney 293T cells (HEK293T cells) (referred to herein as IL-10 cells) coding murine IL-10. Next, IL10-EVs (including exosomes and microvesicles) were separated from the culture supernatants using an ultracentrifugation method. To verify the feasibility of this method, we first transfected *ZsGreen*-tagged IL-10 plasmids into HEK293T cells. As anticipated, fluorescence could be observed using fluorescence microscope only in transfected cells but not in the untreated cells (Figure 1B). Western blotting assays also showed that IL-10 was specifically expressed in IL-10 cells (Figure 1C). We next isolated the EV-like particles from untreated and IL-10 transfected cell culture supernatants and primarily focused on the characterization of their size and morphology, characteristic protein markers, and IL-10 content, although there also possibly exist various RNA types such as IL-10 mRNA in the isolated EVs.[38] Each type of particle isolated through sequential

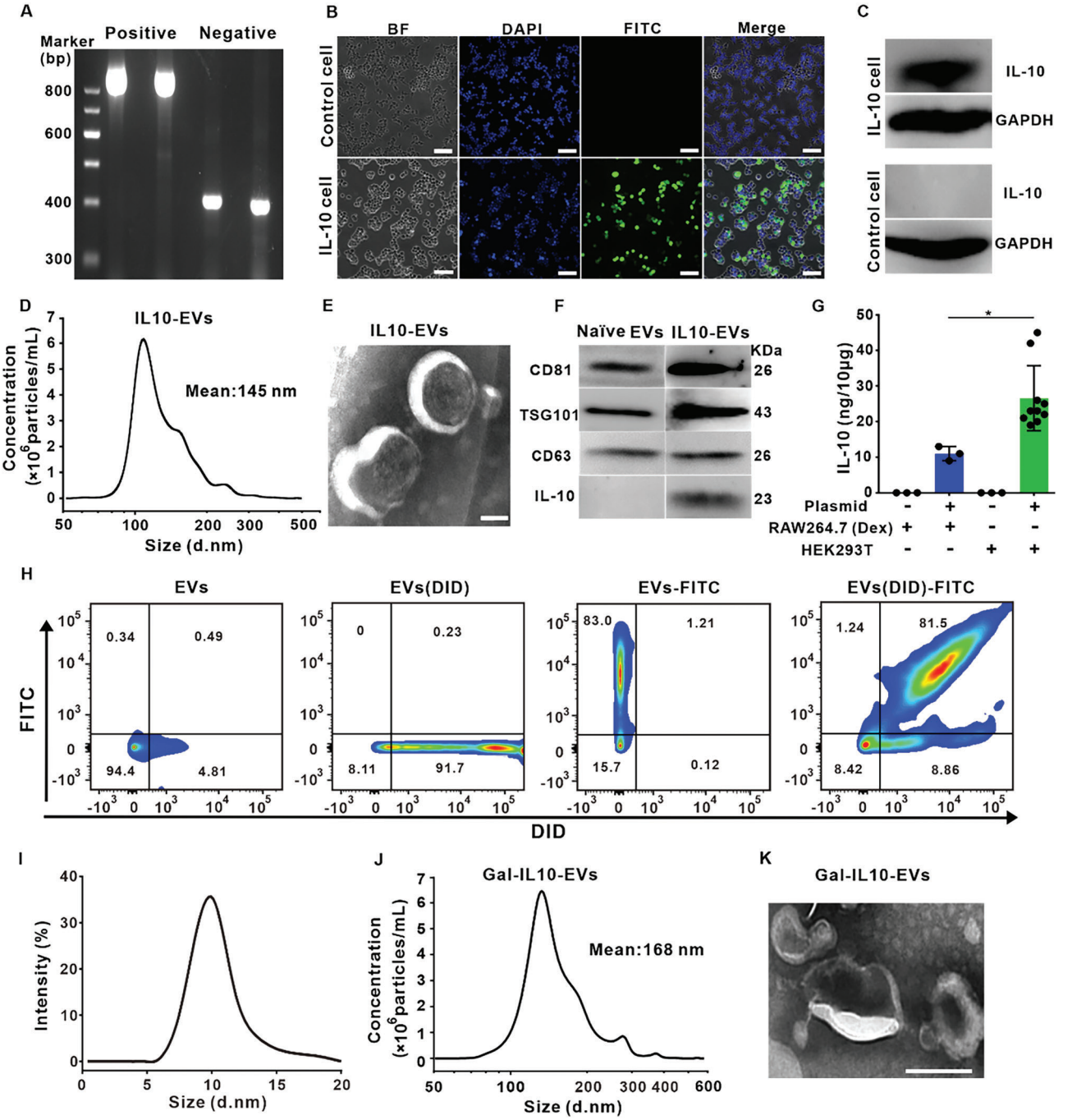

Figure 1. Preparation and characterization of Gal-IL10-EVs. A) Colony PCR validation of target gene (IL-10 gene) contained in plasmids carried by *Escherichia coli* Top10 strains. The murine IL-10 expression plasmid was used as a positive group whereas the identical empty plasmid was treated as a negative group. B) HEK293T cells were transfected with *ZsGreen*-tagged *IL-10* plasmids, the expression of *ZsGreen-IL-10* was observed by fluorescence microscope. Untreated HEK293T cells were used a control cells. Scale bar, 100 μm. C) Western blotting analysis of target protein (IL-10) in IL-10 cells and untreated HEK293T cells (control cells). D) Size distribution of particles derived from IL-10 cells detected by NTA. E) Representative TEM image of particles derived from IL-10 cells. Scale bar, 50 nm. F) Western blotting analysis of EVs-associated markers (CD81, TSG101, CD63) and target protein (IL-10) in particles derived from untreated HEK293T cells and IL-10 cells. G) ELISA analysis of IL-10 in EVs derived from transfected HEK293T cells. Transfected RAW264.7 macrophages with dexamethasone (Dex) stimulation and untreated cells (HEK293T and RAW264.7 macrophages)-derived EVs were treated as control groups ($n = 3$ or 10). H) Flow cytometry analysis of galactose-modified extracellular vesicles. FITC as a surrogate model drug. I) Size distribution of DSPE-PEG-Gal measured by dynamic light scatting. J) Size distribution of Gal-IL10-EVs detected by NTA. K) Representative TEM image of Gal-IL10-EVs. Scale bar, 100 nm. Data were represented the mean ± S.D. Statistical significance was calculated via one-way ANOVA with Turkey's test: ns = no significance, *p <0.05, **p <0.01, ***p <0.001, ****p <0.0001.

purification was also tested via nanoparticle tracking analysis (NTA). Figure S1A (Supporting Information); and Figure 1D show that the particles derived from normal cells and IL-10 cells had similar diameters ranging from 50 to 500 nm, with mean diameters of 145.6 ± 3.0 and 145.3 ± 1.3 nm, respectively. In addition, the intact round-shaped vesicles with a double-membrane structure were visible by transmission electron microscopy (TEM) (Figure S1B (Supporting Information); and Figure 1E). Western blotting analysis showed that both isolated particles expressed common EV-associated proteins including TSG101, CD81, and CD63. At the same time, IL-10 could only be detected in EVs derived from IL-10 cells (Figure 1F). The successful isolation of IL10-EVs was generally consistent with the typical characterization of EVs previously reported.[38,42] Enzyme-linked immunosorbent assay (ELISA) also showed that IL-10 plasmid transfection resulted in a significant increase IL-10 concentration in EVs derived from different cell types (Figure 1G).

After validating the feasibility of preparing IL10-EVs by this genetic engineering approach, we next modified IL10-EVs by inserting galactose (Gal) targeting moieties to enhance the accumulation of IL10-EVs in inflammatory macrophages infiltrating in the colonic lamina propria. To do so, Gal was conjugated to 1, 2-Distearoyl-*sn*-glycero-3-phosphoethanolamine-Polyethyleneglycol2000-Amino (DSPE-PEG-NH_2) to generate 1,2-Distearoyl-*sn*-glycero-3-phosphoethanolamine-Polyethyleneglyco l2000-galactose (DSPE-PEG-Gal), which was then inserted in IL10-EVs taking advantage of the membrane anchoring capability of the hydrophobic portion of the DSPE moiety, allowing Gal to be immobilized on the surface of EV membranes. To assess the efficacy of this approach, we used a fluorescence dye, fluorescein isothiocyanate (FITC), as a proxy for galactose and the fluorescent dye, 1,1′-dioctadecyl-3,3,3′,3′-tetramethylindodicarbocyanine, 4-chlorobenzenesulfonate salt (DID) was used to label the membranes of naïve EVs or FITC-EVs, followed by analysis by flow cytometry. As shown in Figure 1H, over 81% of EVs showed both the signals of DID and FITC, suggesting the feasibility of introducing Gal via conjugated DSPE-PEG. The average diameter of DSPE-PEG-Gal detected by dynamic light scattering was about 10 nm (Figure 1I).

The size distribution of Gal-IL10-EVs was evaluated by NTA and the mean diameter of Gal-IL10-EVs was around 168.4 nm, which is just about 20 nm larger than IL10-EVs (Figure 1J). The morphology of Gal-IL10-EVs was observed by TEM (Figure 1K). The typical appearance and the integrity of the EVs remained well after Gal modification.

2.2. In Vitro Cellular Uptake Profile of Gal-EVs

Macrophage galactose-type lectins (MGLs) are C-type galactose receptors, which are selectively expressed by immature dendritic cells and macrophages, and are expressed at high levels on the surface of activated subpopulations under inflammatory conditions.[43] After confirmation of the successful galactose modification on EVs, the cellular uptake efficacy of Gal-EVs was then evaluated. In addition, to determine if the uptake of Gal-EVs by macrophages was mediated by MGLs. We also measured the internalization efficiency of Gal-EVs in the presence of free galactose, which competitively binds to the MGLs on the surface of macrophage. Naïve EVs and Gal-EVs were labeled with 3,3′-dioctadecyloxacarboc-yanine perchlorate (DIO), followed by incubation with RAW264.7 cells for 4 h. **Figure 2**A showed that the mean fluorescence intensity of Gal-EVs treated macrophages was significantly higher than that in cells incubated with EVs and galactose + Gal-EVs. Also, there was no significant difference between the EVs group and the galactose + Gal-EVs group. These suggest that internalization of Gal-EVs by cells may not depend exclusively on MGLs, but galactose-modified extracellular vesicles can significantly improve the targeted cellular uptake.

2.3. In Vitro Antioxidant and Anti-Inflammatory Activity of Gal-IL10-EVs

The inflamed colon is characterized by elevated levels of reactive oxygen species (ROS). The dysregulated ROS can lead to oxidative stress, damaging biomolecules like DNA, proteins, and lipids.[44,45] IL-10 prevents the accumulation of dysfunctional mitochondria and production of ROS by inducing mitochondrial autophagy.[46] Therefore, we next investigated the antioxidant capacity of Gal-IL10-EVs by coculturing RAW264.7 macrophages with Gal-IL10-EVs for 24 h after lipopolysaccharides (LPS) stimulation for 4 h. At the same time, LPS-treated cells without Gal-IL10-EVs treatment were used as a positive control, whereas cells without LPS or EVs treatment was used as a negative control. Intracellular ROS was detected using an oxidation-sensitive fluorescent probe 2', 7'-dichlorodihydrofluorescein diacetate (DCFH-DA), which was assessed by fluorescence microscope observation and spectrophotometer. In macrophages treated with Gal-IL10-EVs, the level of ROS was significantly decreased compared to the positive control (Figure 2B). Spectrophotometer results confirmed these observations (Figure 2C), suggesting that Gal-IL10-EVs could efficiently decrease LPS-induced ROS in activated macrophages and exhibited strong antioxidant activity.

IBD leads to infiltration of inflammatory macrophages and overexpression of numerous proinflammatory cytokines. Previous studies have demonstrated that IL-10 inhibits the transcription of Nuclear Factor Kappa B (NF-κB) initiated proinflammatory factor genes mainly by suppressing the activation of IκB kinase or DNA binding to NF-κB.[47,48] In this study, ELISA assays were used to verify the effect of Gal-IL10-EVs on the secretion of main proinflammatory cytokines (IL-12p70, IL-6, TNF-α, and IL-1β) from RAW264.7 macrophages after LPS-stimulation. As shown in Figure 2D,E, the suppression effect of proinflammatory cytokine secretion from activated macrophages by Gal-IL10-EVs is dose- and incubation time-dependent (24 h for Figure 2D and 48 h for Figure 2E). It was shown that the concentration of proinflammatory cytokines in the supernatant of RAW264.7 macrophages treated with LPS only was much higher than that of negative control cells without LPS treatment, and these results were in agreement with that presented in previous studies.[49,50] In stark contrast to these observations, much less amounts of IL-12p70, IL-6, TNF-α, and IL-1β were detected in the supernatants of Gal-IL10-EVs-treated cells. More importantly, the expression of IL-12p70, IL-6, TNF-α, and IL-1β were down-regulated in macrophages pretreated with Gal-IL10-EVs in a dose-dependent manner. Gal-IL10-EVs showed significantly

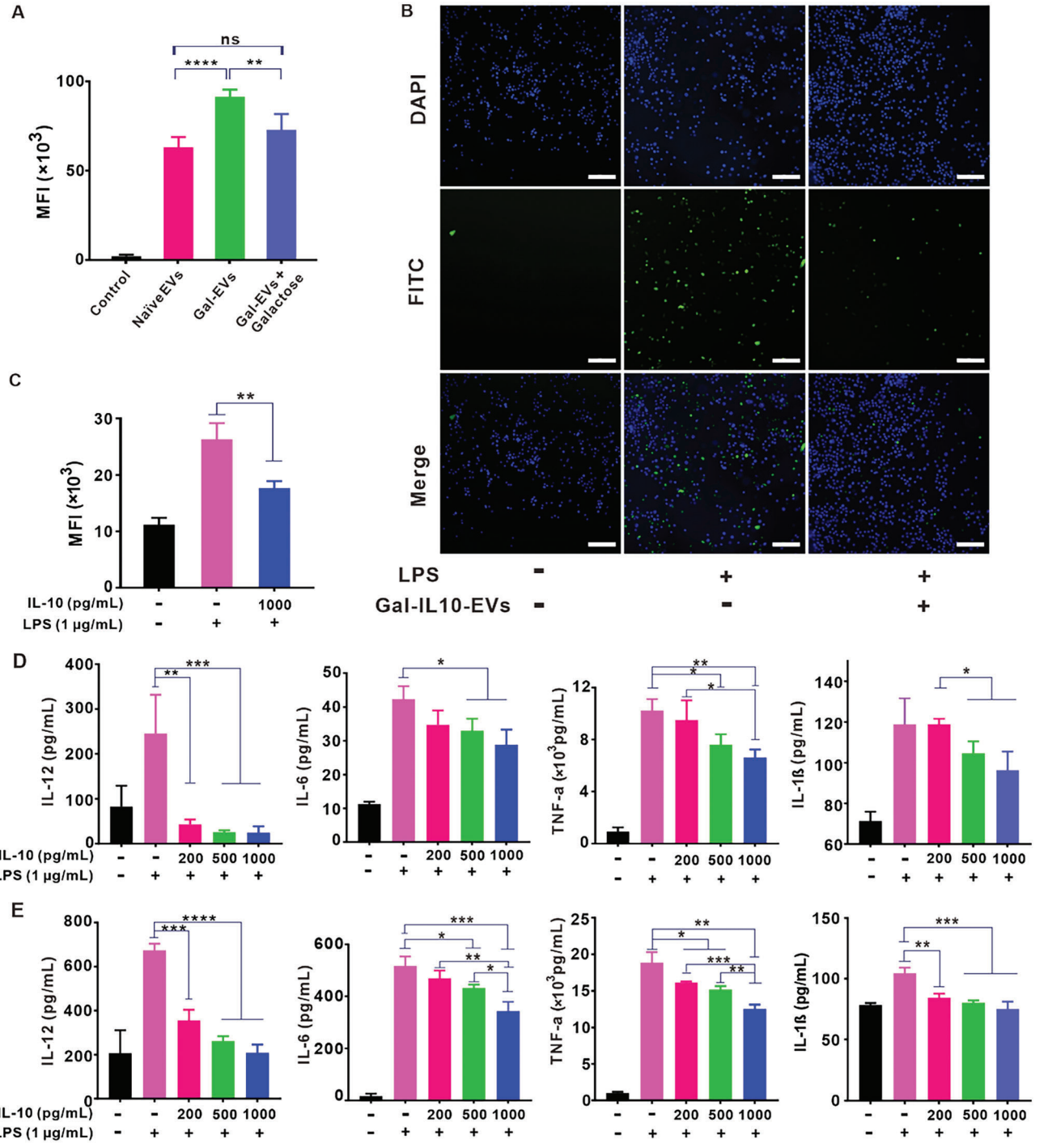

Figure 2. In vitro cellular internalization, antioxidant activities, and anti-inflammatory properties of Gal-IL10-EVs. A) Mean fluorescence intensities (MFIs) of RAW264.7 macrophages after co-incubation for 4 h with DIO-labeled EVs and Gal-EVs that are modified with or without galactose. B) Fluorescence images of RAW264.7 macrophages treated with Gal-IL10-EVs showing intracellular ROS (DCFH-DA). RAW264.7 macrophages were incubated with Gal-IL10-EVs for 24 h after to LPS stimulation for 4 h in Gal-IL10-EVs group. The intracellular ROS profiles were determined using DCFH-DA as a probe. Scale bar represents 100 μm. C) MFIs of RAW264.7 macrophages treated with Gal-IL10-EVs showing intracellular ROS (DCFH-DA) signals. In vitro anti-inflammatory activities of Gal-IL10-EVs at D) 24 and E) 48 h, respectively. The concentrations of proinflammatory cytokines (IL-12p70, IL-6, TNF-α, and IL-1β) were quantified by using the corresponding ELISA kit. The suppression effect of proinflammatory cytokines including IL-12p70, IL-6, TNF-α, and IL-1β secreted from activated macrophages after treatment by Gal-IL10-EVs for 24 h (D) or 48 h (E) ($n = 3$). Data were presented as mean ± S.D. Statistical significance was calculated via one-way ANOVA with Turkey's test: ns = no significance, *$p < 0.05$; **$p < 0.01$; ***$p < 0.001$; ****$p < 0.0001$.

better anti-inflammatory activities at 48 than 24 h. These data proved that Gal-IL10-EVs could potentially provide a long-acting therapeutic effect for prevention or alleviation of inflammatory diseases. Further work is required to better understand the exact mechanisms of Gal-IL10-EVs, but a working hypothesis is that although the particles are up taken primarily via a galactose-mediated pathway. The interleukin receptors which are known to also be endocytosed could be present in some amount in the endocytic vessels and may still be able to exert signaling once these are degraded and IL-10 is released.[51] Other examples have been described of exogenous IL-10 EV systems that were endocytosed first[38] and exocytosis of endogenous IL-10 to exert signaling has also been reported.[52]

2.4. In Vivo Distribution of Gal-IL10-EVs

Administering drugs by oral route is preferred since it offers safety and patient compliance. However, the harsh environment of the gastrointestinal tract, including strong acidity, digestive enzymes, and bacterial species, is likely to destabilize EVs and degrade the IL-10 payload. In addition, the accumulation of Gal-IL10-EVs in the inflamed colon is essential for exerting therapeutic effect against IBD. To keep the stability of Gal-IL10-EVs in gastrointestinal tract and to achieve precisely release payload in the colonic lumen, Gal-IL10-EVs were embedded in chitosan/alginate hydrogel (C/A) at the ratio of 7: 3 (alginate: chitosan, wt/wt), because this combination has good biocompatibility[53] and could well protect EV in harsh conditions in stomach but become collapsed in colon, resulting in release of Gal-IL-10 EVs,[54] although further investigation is required to elucidate the mechanism of collapse. Other advantages of the C/A gel include that the gelation process can be easily initiated by multivalent cations and also C/A has slight inhibitory effect on inflammatory cells.[55] The preparation of C/A, unlike other common biomaterials for enteric coating such as Eudragit line, does not involves using organic solvent. Western blotting assays were next used to test if characteristic protein in Gal-IL10-EVs (C/A) could be well preserved after incubation with simulated gastric fluid (SGF) for 2 h. As shown in **Figure 3**A, in the presence of coating of the C/A hydrogel group, the associated proteins were well protected.

In contrast, in the unprotected group, EVs-related markers (CD81 and TSG101) as well as the anti-inflammatory protein IL-10 were not observed likely because they were fully degraded by gastric acid or pepsin. The cargo release kinetics of the gel when it was incubated in SGF and simulated intestinal fluid (SIF) is shown in Figure 3B. Almost no release was observed in SGF within 2 h, which is much less than the gastric transit time, while at least 80% was released within 4 h in SIF, indicating that C/A hydrogel as a qualified protective coating can protect Gal-IL10-EVs in SGF but release cargo in SIF.

To determine the accumulation profile of Gal-IL10-EVs in colon, 1, 1′-dioctadecyl-3,3,3′,3′-tetramethylindotricarbocyanine iodide (DIR) as a near infrared probe was used to label Gal-IL10-EVs. Mice with IBD were orally administered DIR-labeled Gal-IL10-EVs (0.6 mg protein per kg body weight) embedded in C/A hydrogel, followed by near-infrared fluorescence (NIRF) imaging. Excised tissues from IBD mice treated by phosphate buffer solution (PBS) were used as a control (Figure 3C). 12 h after oral administration of DIR-labeled Gal-IL10-EVs (C/A), the strongest residual NIRF intensity was still seen in the stomach, whereas a weak NIRF signal was detected in cecum and colon. Furthermore, the diffuse NIRF signal was only observed in colon at 24 h, suggesting that C/A hydrogel is likely to protected cargo passes through the stomach but collapse due to pH in the diseased colon. After 48 h of oral administration, the Gal-IL10-EVs was substantially excreted. The quantification of the corresponding average fluorescence in colon revealed the NIRF signal at 24 h was significantly higher than that in 12 or 48 h (Figure 3D), in agreement with Figure 3C. We also examined the distribution of DIR-labeled Gal-IL10-EVs in the heart, liver, spleen, lung, and kidney. As shown in Figure 3E, no obvious NIRF signal was observed in main organs with treatment by Gal-IL10-EVs (C/A), since the majority of NIRF signal was likely excreted in feces. This is different from the scenario of tail vein injection where apparent accumulation of Gal-IL10-EVs in the liver site 24 h after injection (Figure S2, Supporting Information). Furthermore, as shown in Figure S3 (Supporting Information), quantitative analysis in the main organs showed that the average fluorescence intensity at 48 h after oral administration was greater than that at 12 or 24 h, with slightly higher accumulation in the liver and spleen, likely due to a high expression level of sialoglycoprotein receptors on the surface of hepatocytes, which can bind to galactose-containing nanoparticles and mediate uptake by cells.[56] Altogether, these findings suggest that oral administration of DIR-labeled Gal-IL10-EVs (C/A) can maintain stability in the gastrointestinal tract and ensure the release and accumulation of DIR-labeled Gal-IL10-EVs at the target site.

2.5. In Vivo Therapeutic Effect of Gal-IL10-EVs (C/A) Against IBD

Encouraged by these above results, we further investigated whether Gal-IL10-EVs could exert therapeutic effect against IBD in vivo. Twenty male C57BL/6 mice were randomly divided into five groups including: (I) healthy control group given PBS only, (II) DSS control group given PBS with 4% DSS, (III) Naïve EVs group given PBS with 4% DSS and normal EVs, (IV) IL10-EVs group given PBS with 4% DSS and IL10-EVs, and (V) Gal-IL10-EVs group given PBS with 4% DSS and Gal-IL10-EVs. Different forms of EVs were all encapsulated in the C/A hydrogel. **Figure 4**A shows the scheme for the experimental investigation exploring the potential of various EVs to alleviate IBD. The administration groups were given a dose of 0.3 mg protein EVs per kg body weight on day 3 and 5 per mouse. The body weight of the mice was monitored and recorded daily. On day 7, after collecting blood, mice were sacrificed and organs were excised for following evaluation. As shown in Figure 4B, the healthy control group slightly gained weight, whereas the DSS control group and the naïve EVs group showed significant body weight loss. Interestingly, treatment with IL10-EVs or Gal-IL10-EVs mitigated the weight loss. Furthermore, the Gal-IL10-EVs group exhibited the smallest body weight loss among the all groups, and there was statistically significant difference between the Gal-IL10-EVs group and DSS control group as well as the naïve EVs group.

The spleen is a crucial immune organ where immune cells proliferate and spleen weight can increase once strong

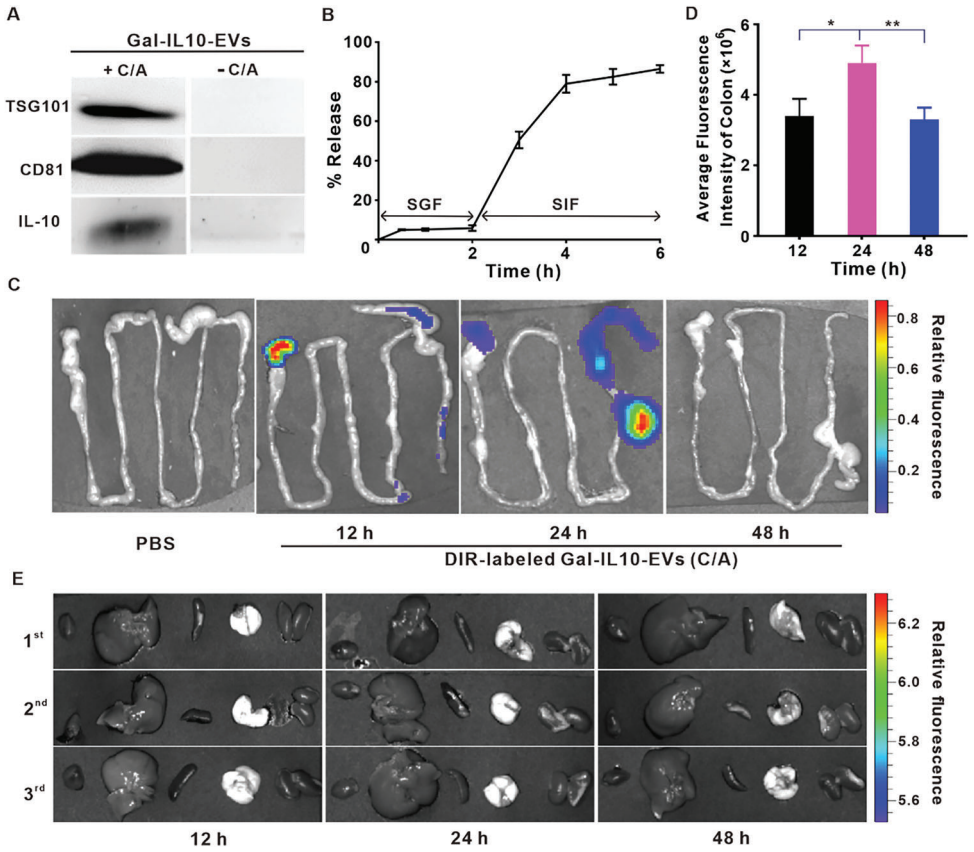

Figure 3. In vivo biodistribution of Gal-IL10-EVs. A) Western blotting analysis of EVs-associated markers (CD81 and TSG101) and target protein (IL-10) in Gal-IL10-EVs with or without the chitosan/alginate hydrogel protection after incubation with simulated gastric fluid (SGF) for 2 h. B) Cumulative collapse kinetic of chitosan/alginate gel and release of cargo in the presence of simulated gastric fluid (SGF) and simulated intestinal fluid (SIF). C) Fluorescence images of the IBD mice gastrointestinal tract showing in vivo bio-distribution of orally administered DIR-labeled Gal-IL10-EVs (C/A) at different time points (12, 24, and 48 h), IBD mice with administration of PBS were used as a control group. D) Quantification of average fluorescence intensities of the colon from mice receiving the oral administration of DIR-labeled Gal-IL10-EVs (C/A) at different time points (12, 24, and 48 h). E) Fluorescence images of major organs (heart, liver, spleen, lung, kidney) of the mice with IBD showing in vivo bio-distribution of orally administered DIR-labeled Gal-IL10-EVs (C/A) at different time points (12, 24, and 48 h). Data were represented the mean ± S.D ($n = 3$). Statistical significance was calculated via one-way ANOVA with Turkey's test: ns = no significance, *$p < 0.05$; **$p < 0.01$; ***$p < 0.001$; ****$p < 0.0001$.

inflammation occurs.[57] Thus changes in its weight can indirectly reflect the inflammation level. As shown in Figure 4C, the average spleen weight increased remarkably after treatment with DSS for 7 days, while the treatment groups prevented the increase in spleen weight, especially for the Gal-IL10-EVs group, demonstrating that oral administration of IL-10 could prevent DSS-associated splenomegaly. In addition, IL10-EVsand Gal-IL10-EVsprevented DSS-induced progression of disease as evidenced by increased colon length at day 7 (Figure 4D). The disease activity index (DAI), which includes the parameters of weight loss, hemafecia and stool consistency,[58] is commonly used to reflect the severity of inflammatory. The recorded scores indicated that the DSS control group and the naïve EVs group had the highest DAI, whereas the Gal-IL10-EVs group had the lowest DAI among all the experimental group with statistical significance at day 7 (Figure S4A, Supporting Information). The severity of acute inflammatory disease is also related to the level of circulating proinflammatory cytokines.[59] We found that the main proinflammatory cytokines, IL-12p70, IL-6, and IL-1β were significantly increased in the DSS control group compared with the healthy control group. The Gal-IL10-EVs group showed greater reduction of proinflammatory cytokines secretion than the other dosing groups (Figure 4E–G), consistent with previous reports.[60,61] In addition, chitosan has also been shown a therapeutic effect on colonic inflammatory cells.[62] This could explain that the naïve EVs group also seems to slightly inhibit the production of proinflammatory factors by inflammatory macrophages.

Hematoxylin and eosin (H&E)-stained colon cryosections obtained from the different groups were evaluated for histological structure changes (Figure 4H). We found that the colon tissue sections from the healthy control group exhibited unremarkable histological characteristics without any noticeable mucosal and submucosal changes, while the mucosal structures of DSS control and Naïve EVs-treated mice were significantly altered, including damaged colonic epithelial layers, the accumulation of inflammatory macrophages, and disruption of the crypt structures. IL10-EVs-treated mice showed histological features reflecting moderate damaged. The colonic histological structure of Gal-IL10-EVs treated-mice were significantly ameliorated, confirming good therapeutic outcome. When these changes

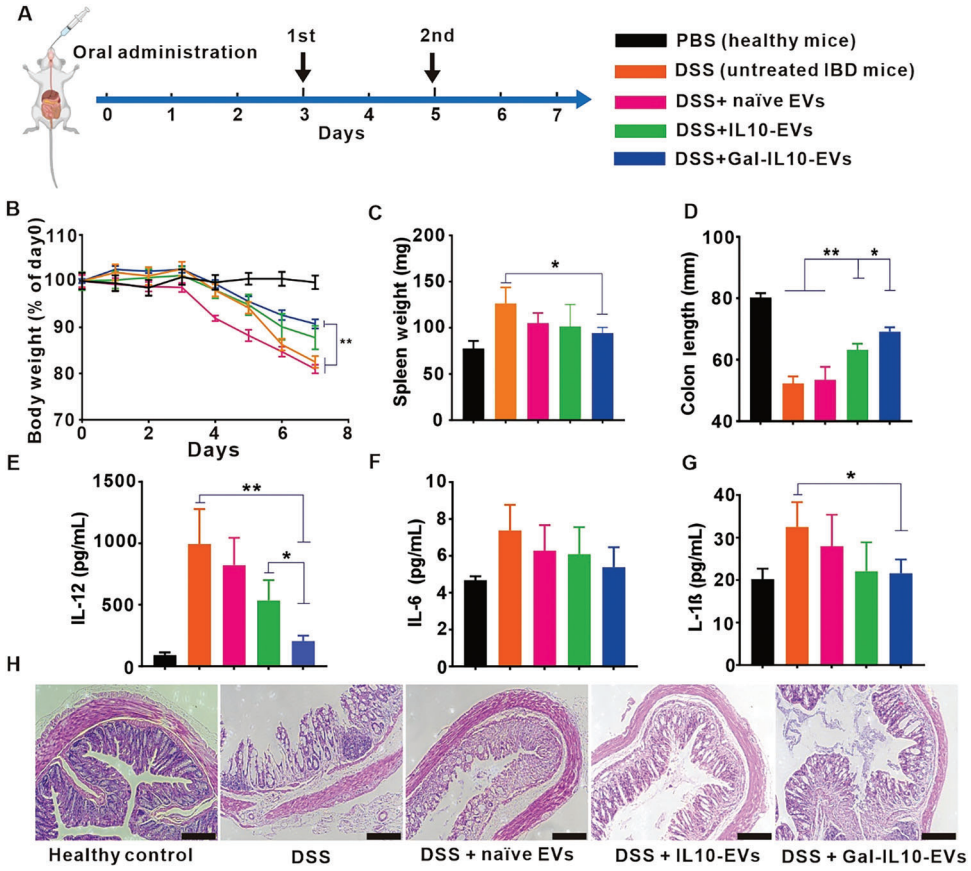

Figure 4. In vivo therapeutic effect of Gal-IL10-EVs (C/A) against IBD via oral route. A) Scheme for EV administration and DSS treatment. Mice were feed with PBS or DSS solution (4%, w/v) for 7 days. On day 3 and day 5, mice were orally administered with PBS or different EVs as indicated (0.3 mg protein kg^{-1}). B) Variations of body weight over time, normalized to the percentage of the day-zero body weight. C) Spleen weight. D) Colon length and E–G) levels of colonic inflammatory cytokines after blood or organs were collected on day 7. H) H&E-stained colon sections. Scale bar represents 200 µm. Data were represented the mean ± S.D ($n = 4$). Statistical significance was calculated via one-way ANOVA with Turkey's test: ns = no significance, $*p < 0.05$; $**p < 0.01$; $***p < 0.001$; $****p < 0.0001$.

were quantified using a colon damage scoring system, the DSS group had the highest histological score among all the groups, whereas the Gal-IL10-EVs group had a much lower score than the other groups involving the treatment of DSS (Figure S4B, Supporting Information). These results imply that the treatment of Gal-IL10-EVs (C/A) have the capacity to alleviate inflammatory responses in colon tissues.

2.6. Biocompatibility of Gal-IL10-EVs

We next evaluated the biocompatibility of Gal-IL10-EVs in vivo and in vitro. We first tested the in vitro cytotoxicity of Gal-IL10-EVs against RAW264.7 macrophages and NIH-3T3 cells (normal cell) using the Cell Counting Kit-8 assay. Gal-IL10-EVs did not exhibit cytotoxicity against either of these cell lines, at protein concentration up to 20 µg mL^{-1} (**Figure 5**A). Instead, they demonstrated a pro-proliferative effect, and EVs have been reported to be associated with cell proliferation.[63] Next, we orally administrated Gal-IL10-EVs (C/A) to mice and assessed the systemic toxicity. On day 0, six C57BL/6 mice were randomly divided into two groups, one as a healthy control group and the other as an experimental group (0.6 mg protein per kg body weight). Mice in both groups displayed gradual increases in their body weight, and there was no statistically significant difference in body weight was found between the healthy control group and the Gal-IL10-EVs (C/A)-treated group (Figure 5C). The organ indexes of the major organs, spleen/body weight ratio, and colon length were examined. As presented in Figure 5B,D,E, similarly, no abnormal changes were observed in the treatment group. After 7 days of oral drug administration, blood sample was collected. A complete blood count revealed that there was no obvious difference between the two groups for any of the parameters examined in Figure 5H, including mean corpuscular hemoglobin (MCH), monocyte number, platelet distribution width (PDW) and others. In addition, since oral administration of Gal-IL10-EVs (C/A) caused accumulation in the liver and kidney (Figure S3, Supporting Information), we assessed the potential toxicities of Gal-IL10-EVs (C/A) to liver and kidney by evaluating aspartate aminotransferase (AST) as the main serological index of liver function and uric acid (UA) that reflects kidney function. None of the mice receiving Gal-IL10-EVs (C/A) treatment exhibited any significant difference with the healthy control group (Figure 5F,G).

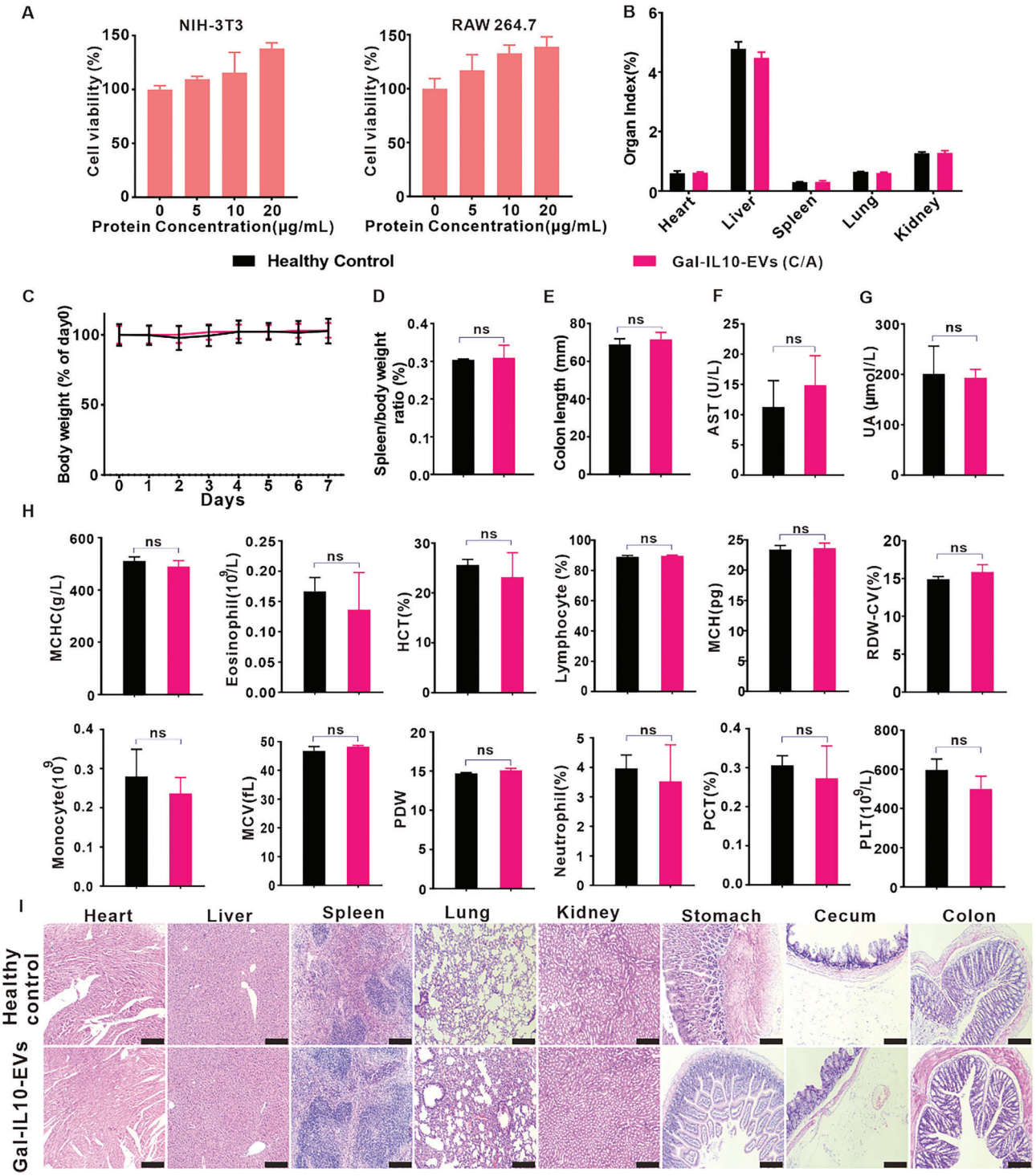

Figure 5. Biocompatibility of Gal-IL10-EVs. A) Viability of NIH-3T3 cells and RAW264.7 macrophages after treatment with Gal-IL10-EVs at different concentrations of Gal-IL10-EV ($n = 4$). B) Organ index (organ weight/body weight), C) body weight, D) spleen weight/body weight ratios, E) colon length, F) liver function, and G) kidney function. H) The complete blood analysis. I) H&E staining of the major organs and different sections of the GIT (stomach, cecum, and colon) after mice were orally gavaged by PBS or Gal-IL10-EV (C/A) (0.6 mg protein per kg body weight) on day 0. Scale bar represents 200 μm. Data were represented the mean ± S.D ($n = 3$). Statistical significance was calculated via one-way ANOVA with Turkey's test: ns = no significance, $*p < 0.05$; $**p < 0.01$; $***p < 0.001$; $****p < 0.0001$.

Moreover, after examining the major organs (heart, liver, spleen, lung, and kidney) and gastrointestinal tract tissues (stomach, cecum, and colon) by hematoxylin and eosin (H&E) staining (Figure 5I), we did not find any evidence of histopathological damage in the experimental group compared to the healthy control group. Therefore, Gal-IL10-EVs appear to have a favorable safety profile after oral administration, at least in mice.

3. Conclusion

In summary, a nanoplatform for oral targeted protein delivery for IBD treatment was developed by engineering EVs decorated with galactose, subsequently coated by chitosan/alginate hydrogel to protect IL-10 in the stomach. The coating of Gal-IL10-EVs (C/A) could become collapsed and release Gal-IL10-EVs in colon. The presence of galactose and extracellular vesicles enabled IL-10 targetable to the inflammatory macrophages through galactose receptors. In vitro studies showed that Gal-IL10-EVs possess potent antioxidant and anti-inflammatory properties. In vivo results showed Gal-IL10-EVs (C/A) could mitigate the symptoms of IBD such as weight loss, shortened colon length, impaired colon tissue, and increased secretion of pro-inflammatory factors. Taken together, Gal-IL10-EVs (C/A) represent a new oral protein delivery system for the treatment of IBD. This approach could hold potential for the delivery of other therapeutic proteins by the oral route.

4. Experimental Section

Cells and Animals: HEK293T cell line and NIH-3T3 cell line (gifted by Prof. Yingjin Yuan's lab in Tianjin University), RAW264.7 macrophage cell line (BeNa Culture Collection, Beijing, China) were cultured in Dulbecco's modified Eagle's medium (DMEM) (Gibco, Grand Island, USA) supplemented with 10% fetal bovine serum (FBS) (YEASEN, Shanghai, China) and 1% penicillin-streptomycin (Gibco, Grand Island, USA). All cell lines were incubated in a humidified atmosphere of 5% CO_2 at 37 °C.

Male C57BL/6 mice (30 ± 2 g, 7–8 weeks) were purchased from Charles River Beijing Co., Ltd (Beijing, China). The mice received care complying with the policy of the National Institutes of Health guide for the care and use of Laboratory animals and animal protocols were approved by Tianjin University Institutional Animal Care and Use Committee (permit number: TJUE-2022-007).

The Validation of Target Gene: The murine IL-10 expression plasmid (CMV-MCS-SV40-puromycin-IL10 plasmid) and the corresponding empty plasmid control (CMV-MCS-SV40-puromycin plasmid) were stored in the *Escherichia coli* Top10 strains (GeneChem, Shanghai, China) and the presence of the target gene (IL-10 gene) was verified using colony PCR following a previous protocol with slight modifications[64] by setting the upstream primer sequences (5' to 3″): CGCAAATGGGCGGTAGGCGT - G and the down-stream primer sequences (5″ to 3'): AACGCACACCG-GCCTTATTC. Upstream and downstream primers were made by Genewiz (Suzhou, China)

Cell Transfection: The above murine IL-10 expression plasmid carried by *E. coli* Top10 strain, cultured with Luria–Bertani (LB) liquid medium (with 100 μg mL^{-1} Ampicillin) for 14 h in a 37 °C shaking incubator and extracted and purified with an EndoFree Mini Plasmid Kit II (Tiangen, DP118-02, Beijing, China) according to the manufacturer's instructions. To overexpress murine IL-10 in HEK293T cells, transfections were performed using Lipofectamine 3000 reagent (Invitrogen, CA) with above extracted IL-10 plasmid according to the manufactures' protocols. Briefly, a total of 2.5 μg plasmid, 7.5 μL of Lipofectamine 3000 and 5.0 μL P3000 were mixed with OPTI-MEM (Invitrogen, CA) for the transfection of about 2×10^6 cells, After 6 h of transfection, and the medium was replaced with fresh exosomes-depleted medium. Extracellular vesicles (EVs) including exosomes and microvesicles in the supernatants then were isolated by a centrifugation method. The exosomes-depleted FBS was prepared by ultracentrifugation (120 000 × g, 6 h), and the upper resulting supernatants were passed through a sterile 0.22 μm sterile syringe filter (Biosharp, Hefei, China) and stored at −80 °C for the following experiments.

Purification and Characterization of EVs: The EVs were purified from the cell culture supernatants of HEK293T using a standard protocol with slight modifications.[65] Conditioned cell supernatants were subsequently subjected to sequential centrifugation steps at 300 × g for 15 min, 2000 × g for 20 min, and 4696 × g for 25 min at 4 °C to get rid of floating cells and debris. The resulting supernatants were further passed through a 0.45 μm sterile syringe filter (Biosharp, Hefei, China) and then were ultracentrifuged (Beckman optima XPN-100, Beckman Coulter) at 120 000 × g for 70 min to pellet EVs. The pellet was washed one time and resuspended in sterile PBS (Gibco, Grand Island, USA). The obtained EVs were aliquoted and stored at −80 °C for the following experiments. For the EV size distribution measurement, 1 μL of EVs were dispersed in 1 mL PBS was analyzed by NTA (Particle Metrix-PMX, Malvern, UK). The morphology of the EVs was visualized by a high-resolution transmission electron microscope (TEM) (JEM-2100plus, JEOL, Japan), EVs-associated markers (TSG101, CD63 and CD81), and target protein (IL-10) were identified by western blotting assay. The concentration of IL-10 in EVs was determined by the mouse IL-10 Quantikine ELISA Kit (Solarbio, Beijing, China). The protein concentration of the isolated EVs was quantified using a bicinchoninic acid (BCA) protein assay kit (ThermoFisher Scientific, WI) according to the manufacturer's protocol.

Western Blotting Analysis: Radio immunoprecipitation assay (RIPA) lysis buffer (Beyotime, Shanghai, China) was used to lyse the cells. ExoSimple-Lysis (SWS, Tianjin, China) was used to lyse the EVs and extract the total protein and the protein content were determined using BCA protein assay kit. The protein samples were then mixed with SDS-PAGE loading buffer (Solarbio, Beijing, China) and heated at 100 °C for 5 min, which was subsequently electrophoresed in 10% SDS-PAGE gels and transferred to polyvinylidene difluoride (PVDF) membranes (Solarbio, Beijing, China). After blocking with 5% w/v skim milk (Solarbio, Beijing, China) for 80 min, membranes were incubated with primary antibodies monoclonal mouse anti-TSG101 (K009751P, Solarbio, Beijing, China), anti-CD63 (K007602P, Solarbio, Beijing, China), anti-CD81 (K106869P, Solarbio, Beijing, China), anti-IL10 (K009382P, Solarbio, Beijing, China), anti-GADPH (TA309157, ZSGB-BIO, Beijing, China) overnight at 4 °C. Then membranes were washed and incubated with an antirabbit peroxidase-conjugated secondary antibody (ZB-2301, ZSGB-BIO, Beijing, China). The bands were visualized by ECL luminescence reagent (Biosharp, Hefei, China) and imaged using SH-523 Multifunctional Ultra-Sensitive Imaging System (Shenhua, Hangzhou, China).

Fabrication of Functional Target Molecules: For the synthesis of DSPE-PEG-FITC, 3 mg DSPE-PEG-NH_2 (Ponsure Biological, Shanghai, China) was first dissolved in pH = 10, 0.1 ml L^{-1} $NaHCO_3$ solution (5 mL), and then 2.8 mg FITC (Aladdin, Shanghai, China) in 0.1 mL DMSO solution was slowly added dropwise, then subjected to stirring in dark overnight, dialysis to removal unconjugated compounds, freeze-dry and storage in −20 °C for future use.

Preparation of Gal-EVs: To form galactose-inserted EVs, the EVs solution (1 mg mL^{-1}) was stirred for 30 min with DSPE-PEG-galactose (0.1 mg mL^{-1}), enabling DSPE-PEG-galactose inserting into EVs membranes following a previously reported protocol.[40] Then the mixture was ultracentrifuged (120 000 × g, 70 min) to remove free DSPE-PEG-galactose and then stored in sterilized PBS solution for subsequent experiments.

Transmission Electron Microscope: The isolated fresh EVs or engineered EVs were dripped onto a 300-mesh carbon-coated grid and absorbed for 2 min and then the grid was negatively stained with 2% phosphotungstic acid for 1 min at room temperature. A JEM-2100plus transmission electron microscope (JEOL, Tokyo, Japan) at an accelerating voltage of 120 KV was employed to observe the samples.

Labeling of EVs: EVs were labeled with the fluorescent lipophilic dyes. DID (Solarbio, Beijing, China), DIR (Solarbio, Beijing, China), and DIO

(Solarbio, Beijing, China) were dissolved in DMSO. To obtain DID-labeled or DIR-labeled EVs, 10 μM dye solution was added to EVs (1 mg mL^{-1}), and the mixture was then incubated for 30 min at 37 °C. The labeled EVs were washed in PBS by centrifugation at 120 000 × g, 4 °C for 70 min to remove the free dyes. The obtained EVs were aliquoted and stored at −80 °C for the further use.

Targeted Modification Characterization: To verify that the DSPE-PEG-Gal molecules could be successfully anchored on the surface of the extracellular vesicle membrane, the fluorescent dye fluorescein isothiocyanate FITC was chosen as the model drug, and the successful anchoring was detected by flow cytometry. The EVs embedded with DSPE-PEG-FITC (FITC-EVs) were first prepared and then labeled with the fluorescent lipophilic dye DID. After labeling, sterile PBS buffer was added at 120 000 g and centrifuged at 4 °C for 70 min to remove free molecules. The supernatant was then discarded, and the precipitate was resuspended in sterile PBS buffer and assayed by flow cytometry. The results were analyzed using the software FlowJo. EVs unlabeled with DID dye and DSPE-PEG-FITC were used as negative controls, and EVs labeled with only DID dye or DSPE-PEG-FITC were used as single positive controls.

Quantification of In Vitro Cellular Uptake of Gal-EVs: RAW264.7 macrophages were seeded in 48-well plates at a density of 1×105 cells per well and incubated overnight. RAW264.7 macrophages were then divided into 4 groups including control group, EVs group (protein concentration: 20 μg mL^{-1}), Gal-EVs group (protein concentration: 20 μg mL^{-1}), Galactose + Gal-EVs group (Pretreatment with 200 μg mL^{-1} galactose 3 h, Gal-EVs protein concentration: 20 μg mL^{-1}). EVs and Gal-EVs were all labeled by DIO dyes. After incubation for 4 h, cells were washed with PBS for 3 times and collected for further use. And cells were lysed cells and centrifuged to collect supernatant. Fluorescence intensity was quantified using a spectrophotometer (Excitation Wavelength: 480 nm, Emission Wavelength: 510 nm). In this experiment, HEK293 T cell membrane-forming nanoparticles that was synthesized by a lipid extruder with 100 nm membrane and has similar size as that of EVs were used as a surrogate for EVs.

In Vitro Anti-inflammatory Activity of Gal-IL10-EVs: RAW264.7 macrophages were seeded in 48-well plates at a density of 1×10^5 cell per well and incubated with different concentrations of Gal-IL10-EVs (IL-10 concentration: 200, 500, and 1000 pg mL^{-1}, respectively). After incubation for 24 and 48 h, cells were washed with PBS for 3 times, and then stimulated with lipopolysaccharide (LPS, 055:B5, 1 μg mL^{-1}) (Biosharp, Hefei, China) for 4 h. Subsequently, the supernatants were collected, and the concentrations of inflammatory factors (TNF-α, IL-6, and IL-12p70) were quantified by their corresponding enzyme-linked immunosorbent assay (ELISA) kits following the manufacture's procedure. IL-1β cytokine concentration were measured in the same way as above, but the LPS stimulation time was extended to 24 h. RAW264.7 macrophages in the absence of Gal-IL10-Evs and LPS were used as a negative control group, while LPS stimulated cells were treated as a positive control group.

Detection of Intracellular ROS: Intracellular ROS was detected using an oxidation-sensitive fluorescent probe 2', 7'-dichlorodihydrofluorescein diacetate (DCFH-DA). RAW264.7 macrophages were divided into 3 groups including (I) Negative control group, (II) Positive control group: LPS stimulation only (1 μg mL^{-1}), (III) Gal-IL10-EVs group: LPS stimulation (1 μg mL^{-1}) + Gal-IL10-EVs (IL-10 concentration: 1000 pg mL^{-1}). RAW264.7 macrophages were incubated with Gal-IL10-EVs (IL-10 concentration: 1000 pg mL^{-1}) for 24 h after to LPS stimulation for 4 h in the Gal-IL10-EVs group, cells were washed with PBS for 3 times. Subsequently, cells were incubated with DCFH-DA (10 μM) at 37 °C for 20 min according to the manufacturer's instructions. Cells were washed with PBS for 3 times and incubated with DAPI for 5 min. Finally, cells were observed and imaged using a fluorescence microscope. Fluorescence intensity was quantified using a spectrophotometer (Excitation Wavelength: 480 nm, Emission Wavelength: 526 nm).

The Release Kinetic of Gal-IL10-EVs: 5,9,14,18,23,27,32,36-octabutoxy-2,3-naphthalocyanine (ONc) encapsulated in Pluronic F127 (F127), termed ONc-F127 was used as a surrogate for Gal-IL10-EVs since ONc-F127 nanoparticle has high absorbance extinction coefficient and easy for quantification using spectrophotometer. To prepare ONc-F127, 1 mg ONc was dissolved in 1 mL dichloromethane chloride and added to 10 mL 10% (wt) F127 aqueous solution. The mixture was stirred for 3 h and then subjected to ultrafiltration at 4 °C twice to remove excessive F127 to make ONc encapsulated F127 micelles with good stability. Chitosan and $CaCl_2$ were dissolved in 1% acetic acid solution, then adjusted to pH 5 using NaOH to obtain a mixture solution of chitosan (0.6 wt%) and $CaCl_2$ (2% w/v). About 20 μL of 0.1 mg (ONc)/mL ONc-F127 was fully mixed in 80 μL sodium alginate solution (1.4 wt%), and two solutions were mixed in equal volumes to form a C/A hydrogel containing F127-ONc. The above gel was placed in SGF for 2 h, then transferred to SIF for 4 h, the process was carried out in a shaker at 37 °C and 100 rpm. The supernatant was taken at 0, 0.5, 1, 2, 3, 4, 5, and 6 h, respectively. And an equal volume of DMSO was added to break up the F127-ONC, and the absorbance was measured at 860 nm using a spectrophotometer.

Double-Gavage Method: The Double-gavage method was adopted from a previous protocol with slight modifications.[66] First, 20 μL Gal-IL10-EVs was thoroughly mixed in 80 μL sodium alginate solution (1.4 wt%). Sodium alginate solution (100 μL), chitosan (0.6 wt%), and $CaCl_2$ (2% w/v) mixed solution (100 μL) were orally administered to mice sequentially using two separate gavage needles within 5–10 s. The hydrogel could be formed when admixing alginate and chitosan at a ratio of 7/3 (wt/wt) in the stomach.

Distribution of Oral Administrated Gal-IL10-EVs (C/A): DIR-labeled Gal-IL10-EVs embedded in chitosan/alginate hydrogel (C/A) were administered to IBD model mice at a protein concentration of 0.6 mg protein per kg body weight via oral route by a double-gavage method. At different timepoints of 12, 24, and 48 h after oral administration, mice were sacrificed to collect gastrointestinal tract and major organs (heart, liver, spleen, lung, and kidney). These organs were imaged using an IVIS spectrum imaging system (PerkinElmer, Spokane, WA).

Distribution of Intravenous Injected Gal-IL10-EVs: DIR-labeled Gal-IL10-EVs were injected to mice at a protein concentration of 0.6 mg protein per kg body weight via intravenous vein injection. 24 h after injection, mice were sacrificed to collect major organs (heart, liver, spleen, lung, and kidney) and then subjected to fluorescence imaging using the IVIS spectrum imaging system (PerkinElmer, Spokane, WA).

In Vivo Therapeutic Effect of Gal-IL10-EVs Against IBD: C57BL/6 male mice were randomly divided into 5 groups including the healthy control group, the DSS control group, the DSS + naïve EVs group, the DSS + IL10-EVs group, and the DSS + Gal-IL10-EVs group. To protect EVs in gastrointestinal tract, they were embedded into a hydrogel, which were prepared by chitosan and alginate at a weight ratio of 3:7 and then administrated to mice by a double-gavage method at a protein concentration of 0.3 mg protein per kg per mouse on day 3 and day 5, respectively. DSS solution (4%, w/v) was freshly prepared and replaced the drinking water of mice every other day. Body weight and activities of mice were monitored daily. On day 7, mice blood was collected for ELISA quantification, then mice were sacrificed, and spleen as well as colon were harvested for weight and length measurements. The colon was divided into two sections, each section of colon is weighed and recorded. The section near the cecum (upstream colon) was used to measure cytokines, the section near the anus (downstream colon) was stained with H.E staining for histological scoring.

The scores of histological colon tissues were recorded as described previously.[67] For the epithelium (E), normal morphology 0; loss of goblet cells 1; loss of goblet cells in large areas 2; loss of crypts 3; and loss of crypts in large areas 4. For the infiltration (I), the criteria were as follows: no infiltration 0; infiltration around the crypt basis 1; infiltration reaching the muscularis mucosae 2; extensive infiltration reaching the muscularis mucosae and thickening of the mucosa with abundant edema 3; and infiltration of the submucosa 4. The total histological score was presented as E + I.

Colon Organ Culture and Cytokine Analysis: Local levels of IL-1β and IL-6 were assessed by first washing upstream colon tissues from different treatment groups with PBS containing 5% penicillin/streptomycin. Colon sections were cultured in serum-free RPMI 1640 medium supplemented with 2% penicillin/streptomycin for 24 h, after which cell-free supernatants were harvested and assayed for cytokine secretion using corresponding ELISA kits. Mice blood samples were collected at the end of experiments by the orbital sinus method. The serum concentrations of IL-12p70 were

quantified by the commercial ELISA kits according to the manufactures' protocols.

Biocompatibility of Gal-IL10-EVs: RAW264.7 macrophages and NIH-3T3 cells were seeded in 96-well plates at a density of 2×10^4 cell per well and cultured overnight. Subsequently, cells were incubated with Gal-IL10-EVs (protein concentration: 5, 10, and 20 μg mL^{-1}) for 24 h, after washed with PBS. These cells were treated with Cell Counting Kit-8 (CCK-8 kit, Solarbio, Beijing, China) (10 μL CCK-8 reagent with 90 μL DMEM medium) at 37 °C for 2 h. The absorbance at 450 nm was measured and untreated cells were used as a negative control. Gal-IL10-EVs embedded in chitosan/alginate hydrogel (C/A) were administered to mice at a protein concentration of 0.6 mg/kg body weight via oral route on day 0. Mouse body weights were recorded daily. At the end of investigation (day 7), blood was collected for complete blood analysis, aspartate aminotransferase (AST) assay, and uric acid (UA) measurements by corresponding commercial kits (Jiancheng, Nanjing, China) according to the manufactures' protocols. Different sections of GIT (stomach, cecum and colon), and major organs (heart, liver, spleen, lung, and kidney) were collected for histology analysis. Organ index = organ weight/body weight. Normal mice were used a negative control group.

Statistical Analysis: Data were presented as mean ± standard deviation (S.D.). Flow cytometry results were analyzed by FlowJo v10. NIR fluorescence images were analyzed by Living Image 4.3 software. Statistical analysis was performed using one-way analysis of variance (ANOVA) with Tukey's post hoc test. Statistical significance was expressed by ns = no significance, *$p < 0.05$, **$p < 0.01$, ***$p < 0.001$, ****$p < 0.0001$. All statistical analysis was performed with GraphPad Prism 8.0 software. All the data supporting the findings of this study are available within the article and its Supporting Information files and from the corresponding author upon reasonable request.

Supporting Information

Supporting Information is available from the Wiley Online Library or from the author.

Acknowledgements

This work was supported by the National Key Research and Development Program (No. 2021YFC2102300) and National Natural Science Foundation of China (No. 32071384), .

Conflict of Interest

The authors declare no conflict of interest.

Author Contributions

J.L. and Y.Z. conceived the project. J.L. carried out most experiments. H.R., C.Z., J.L., Q.Q., L.Z., and N.J. assisted with material synthesis and animal experiments. J.F.L. assisted with manuscript editing. J.L. and Y.Z. performed data analysis and wrote the manuscript. All authors have given approval to the final version of the manuscript.

Data Availability Statement

The data that support the findings of this study are available in the Supporting Information of this article.

Keywords

extracellular vesicles, galactose, inflammatory bowel disease, interleukin 10, oral protein administration

Received: May 13, 2023
Revised: September 11, 2023
Published online:

[1] C. Bauer, P. Duewell, C. Mayer, H. A. Lehr, K. A. Fitzgerald, M. Dauer, J. Tschopp, S. Endres, E. Latz, M. Schnurr, *Gut* **2010**, *59*, 1192.
[2] S. C. Ng, H. Y. Shi, N. Hamidi, F. E. Underwood, W. Tang, E. I. Benchimol, R. Panaccione, S. Ghosh, J. C. Y. Wu, F. K. L. Chan, J. J. Y. Sung, G. G. Kaplan, *Lancet* **2017**, *390*, 2769.
[3] J. R. Turner, *Nat. Rev. Immunol.* **2009**, *9*, 799.
[4] X. Li, C. Lu, Y. Y. Yang, C. H. Yu, Y. F. Rao, *Biomed. Pharmacother.* **2020**, *129*, 110486.
[5] N. J. Simmonds, D. S. Rampton, *Gut* **1993**, *34*, 865.
[6] Y. R. Na, M. Stakenborg, S. H. Seok, G. Matteoli, *Nat. Rev. Gastroenterol. Hepatol.* **2019**, *16*, 531.
[7] L. Jostins, S. Ripke, R. K. Weersma, R. H. Duerr, D. P. Mcgovern, K. Y. Hui, J. C. Lee, L. Philip Schumm, Y. Sharma, C. A. Anderson, J. Essers, M. Mitrovic, K. Ning, I. Cleynen, E. Theatre, S. L. Spain, S. Raychaudhuri, P. Goyette, Z. Wei, C. Abraham, J.-P. Achkar, T. Ahmad, L. Amininejad, A. N. Ananthakrishnan, V. Andersen, J. M. Andrews, L. Baidoo, T. Balschun, P. A. Bampton, A. Bitton, et al., *Nature* **2012**, *491*, 119.
[8] S. Fujino, *Gut* **2003**, *52*, 65.
[9] J. K. Hou, B. Abraham, H. El-Serag, *Am. J. Gastroenterol.* **2011**, *106*, 563.
[10] K. Atarashi, T. Tanoue, K. Oshima, W. Suda, Y. Nagano, H. Nishikawa, S. Fukuda, T. Saito, S. Narushima, K. Hase, S. Kim, J. V. Fritz, P. Wilmes, S. Ueha, K. Matsushima, H. Ohno, B. Olle, S. Sakaguchi, T. Taniguchi, H. Morita, M. Hattori, K. Honda, *Nature* **2013**, *500*, 232-+.
[11] K. M. Das, M. A. Eastwood, J. P. A. Mcmanus, W. Sircus, *N. Engl. J. Med.* **1973**, *289*, 491.
[12] K. H. Katsanos, P. V. Voulgari, E. V. Tsianos, *J. Crohns Colitis.* **2012**, *6*, 735.
[13] C. Lautenschläger, C. Schmidt, D. Fischer, A. Stallmach, *Adv. Drug Delivery Rev.* **2014**, *71*, 58.
[14] B. Xiao, Q. Chen, Z. Zhang, L. Wang, Y. Kang, T. Denning, D. Merlin, *J. Controlled Release* **2018**, *287*, 235.
[15] N. Lugering, T. Kucharzik, H. Stein, G. Winde, A. Lugering, A. Hasilik, W. Domschke, R. Stoll, *Dig. Dis. Sci.* **1998**, *43*, 706.
[16] T. S. Jayme, G. Leung, A. Wang, M. L. Workentine, S. Rajeev, A. Shute, B. E. Callejas, N. Mancini, P. L. Beck, R. Panaccione, D. M. Mckay, *Sci. Adv.* **2020**, *6*, aba4376.
[17] W. Ouyang, A. O'garra, *Immunity* **2019**, *50*, 871.
[18] K. Asadullah, W. Sterry, H. D. Volk, *Pharmacol. Rev.* **2003**, *55*,24
[19] M.-C. Li, *World J. Gastroenterol.* **2004**, *10*, 620.
[20] X. Yang, S. Meng, H. Jiang, T. Chen, W. Wu, *Scand. J. Gastroenterol.* **2010**, *45*, 1168.
[21] T. Lipiäinen, M. Peltoniemi, S. Sarkhel, T. Yrjönen, H. Vuorela, A. Urtti, A. Juppo, *J. Pharm. Sci.* **2015**, *104*, 307.
[22] H. Tilg, H. Ulmer, A. Kaser, G. N. Weiss, *J. Immunol.* **2002**, *169*, 2204.
[23] G. Barbara, *Gut* **2000**, *46*, 344.
[24] Y. Yang, Q. Li, H. C. Ertl, J. M. Wilson, *J. Virol.* **1995**, *69*, 2004.
[25] Y. Yang, F. A. Nunes, K. Berencsi, E. E. Furth, E. Gönczöl, J. M. Wilson, *Proc. Natl. Acad. Sci. USA* **1994**, *91*, 4407.
[26] H. Nakase, K. Okazaki, Y. Tabata, M. Ozeki, N. Watanabe, M. Ohana, S. Uose, K. Uchida, T. Nishi, M. Mastuura, H. Tamaki, T. Itoh, C. Kawanami, T. Chiba, *J. Pharmacol. Exp. Ther.* **2002**, *301*, 59.
[27] L. Steidler, W. Hans, L. Schotte, S. Neirynck, F. Obermeier, W. Falk, W. Fiers, E. Remaut, *Science* **2000**, *289*, 1352.
[28] L. Steidler, S. Neirynck, N. Huyghebaert, V. Snoeck, A. n. Vermeire, B. Goddeeris, E. Cox, J. P. Remon, E. Remaut, *Nat. Biotechnol.* **2003**, *21*, 785.

[29] G. Van Niel, G. D'angelo, G. Raposo, *Nat. Rev. Mol. Cell Biol.* **2018**, *19*, 213.
[30] M. Mathieu, L. Martin-Jaular, G. Lavieu, C. Théry, *Nat. Cell Biol.* **2019**, *21*, 9.
[31] S. Mathivanan, C. J. Fahner, G. E. Reid, R. J. Simpson, *Nucl. Acids Res.* **2012**, *40*, D1241.
[32] H. Valadi, K. Ekström, A. Bossios, M. Sjöstrand, J. J. Lee, J. O. Lötvall, *Nat. Cell Biol.* **2007**, *9*, 654.
[33] L. Balaj, R. Lessard, L. Dai, Y.-J. Cho, S. L. Pomeroy, X. O. Breakefield, J. Skog, *Nat. Commun.* **2011**, *2*, 180.
[34] S. El Andaloussi, I. Mäger, X. O. Breakefield, M. J. A. Wood, *Nat. Rev. Drug Discovery* **2013**, *12*, 347.
[35] S. L. N. Maas, X. O. Breakefield, A. M. Weaver, *Trends Cell Biol.* **2017**, *27*, 172.
[36] O. P. B. Wiklander, M. Á. Brennan, J. Lötvall, X. O. Breakefield, S. El Andaloussi, *Sci. Transl. Med.* **2019**, *11*, eaav8521.
[37] T.-T. Tang, L.-L. Lv, H.-Y. Lan, B.-C. Liu, *Front. Physiol.* **2019**, *10*, 226.
[38] T.-T. Tang, B. Wang, M. Wu, Z.-L. Li, Y. Feng, J.-Y. Cao, D. Yin, H. Liu, R.-N. Tang, S. D. Crowley, L.-L. Lv, B.-C. Liu, *Sci. Adv.* **2020**, *6*, eaaz0748.
[39] X. Pei, X. Zhang, L. Zhang, M. Yuan, L. Sun, F. Yu, B. Wang, J. Zhao, H. He, V. C. Yang, *Chem. Eng. J.* **2021**, *421*, 129774.
[40] R. Yang, J. Xu, L. Xu, X. Sun, Q. Chen, Y. Zhao, R. Peng, Z. Liu, *ACS Nano* **2018**, *12*, 5121.
[41] Y. Liang, L. Duan, J. Lu, J. Xia, *Theranostics* **2021**, *11*, 3183.
[42] A. Eirin, X.-Y. Zhu, A. S. Puranik, H. Tang, K. A. Mcgurren, A. J. Van Wijnen, A. Lerman, L. O. Lerman, *Kidney Int.* **2017**, *92*, 114.
[43] S. J. Van Vliet, E. Saeland, Y. Van Kooyk, *Trends Immunol.* **2008**, *29*, 83.
[44] R. A. Floyd, J. M. Carney, *Ann. Neurol.* **1992**, *32*, S22.
[45] B. S. Baek, H. J. Kwon, K. H. Lee, M. A. Yoo, K. W. Kim, Y. Ikeno, B. P. Yu, H. Y. Chung, *Arch. Pharmacal Res.* **1999**, *22*, 361.
[46] W. K. E. Ip, N. Hoshi, D. S. Shouval, S. Snapper, R. Medzhitov, *Science* **2017**, *356*, 513.
[47] A. J. G. Schottelius, M. W. Mayo, R. B. Sartor, A. S. Baldwin, *J. Biol. Chem.* **1999**, *274*, 31868.
[48] P. Wang, P. Wu, M. I. Siegel, R. W. Egan, M. M. Billah, *J. Biol. Chem.* **1995**, *270*, 9558.
[49] B. Xiao, Z. Xu, E. Viennois, Y. Zhang, Z. Zhang, M. Zhang, M. K. Han, Y. Kang, D. Merlin, *Mol. Ther.* **2017**, *25*, 1628.
[50] M. Zu, D. Xie, B. S. B. Canup, N. Chen, Y. Wang, R. Sun, Z. Zhang, Y. Fu, F. Dai, B. Xiao, *Biomaterials* **2021**, *279*, 121178.
[51] J. Cendrowski, A. Maminska, M. Miaczynska, *Cytokine Growth Factor Rev.* **2016**, *32*, 63.
[52] K. W. Moore, R. De Waal Malefyt, R. L. Coffman, A. O'garra, *Annu. Rev. Immunol.* **2001**, *19*, 683.
[53] D. Aluani, V. Tzankova, M. Kondeva-Burdina, Y. Yordanov, E. Nikolova, F. Odzhakov, A. Apostolov, T. Markova, K. Yoncheva, *Int. J. Biol. Macromol.* **2017**, *103*, 771.
[54] B. o. Xiao, E. Viennois, Q. Chen, L. Wang, M. K. Han, Y. Zhang, Z. Zhang, Y. Kang, Y. Wan, D. Merlin, *ACS Nano* **2018**, *12*, 5253.
[55] A. J. Friedman, J. Phan, D. O. Schairer, J. Champer, M. Qin, A. Pirouz, K. Blecher-Paz, A. Oren, P. T. Liu, R. L. Modlin, J. Kim, *J. Invest. Dermatol.* **2013**, *133*, 1231.
[56] U. Navaneethan, B. A. Lashner, *Clin. Gastroenterol. Hepatol.* **2013**, *11*, 524.
[57] V. Bronte, M. J. Pittet, *Immunity* **2013**, *39*, 806.
[58] D. Turner, C. H. Seow, G. R. Greenberg, A. M. Griffiths, M. S. Silverberg, A. H. Steinhart, *Clin. Gastroenterol. Hepatol.* **2009**, *7*, 1081.
[59] A. Szkaradkiewicz, R. Marciniak, I. Chudzicka-Strugala, A. Wasilewska, M. Drews, P. Majewski, T. Karpinski, B. Zwozdziak, *Arch. Immunol. Ther. Exp.* **2009**, *57*, 291.
[60] M. Zhang, E. Viennois, M. Prasad, Y. Zhang, L. Wang, Z. Zhang, M. K. Han, B. Xiao, C. Xu, S. Srinivasan, D. Merlin, *Biomaterials* **2016**, *101*, 321.
[61] Y. Sun, B. Duan, H. Chen, X. Xu, *Adv. Healthcare Mater.* **2020**, *9*, 1901805.
[62] C. Shi, Y. Zhu, X. Ran, M. Wang, Y. Su, T. Cheng, *J. Surg. Res.* **2006**, *133*, 185.
[63] T. Ma, B. Fu, X. Yang, Y. Xiao, M. Pan, *J. Cell. Biochem.* **2019**, *120*, 10847.
[64] M. Bergkessel, C. Guthrie, P. C. R. Colony, in *Laboratory Methods in Enzymology: DNA* (Ed.: J. Lorsch), Academic Press, Cambridge, MA **2013**, Vol. *529*, pp. 299–309.
[65] G. Casella, F. Colombo, A. Finardi, H. Descamps, G. Ill-Raga, A. Spinelli, P. Podini, M. Bastoni, G. Martino, L. Muzio, R. Furlan, *Mol. Ther.* **2018**, *26*, 2107.
[66] H. Laroui, G. Dalmasso, H. T. T. Nguyen, Y. Yan, S. V. Sitaraman, D. Merlin, *Ann. Gastroenterol. Hepatol.* **2010**, *138*, 843.
[67] X. Sun, S. Somada, K. Shibata, H. Muta, H. Yamada, H. Yoshihara, K. Honda, K. Nakamura, R. Takayanagi, K. Tani, E. R. Podack, Y. Yoshikai, *Ann. Gastroenterol. Hepatol.* **2008**, *134*, 447.